SAND2022-1093C

MELCOR Validation Study on Sodium Pool Fire Model with Comparison to SPHINCS

David L.Y. Louie
Sandia National Laboratories
1515 Eubank SE,
Albuquerque, NM 87123 USA
dllouie@sandia.gov

Mitsuhiro Aoyagi
Japan Atomic Energy Agency
4002 Narita-cho, Oarai, Ibaraki, 311-1393 Japan
aoyagi.mitsuhiro@jaea.go.jp

[leave space for DOI, which will be inserted by ANS]

ABSTRACT

A sodium pool fire in the containment of a sodium-cooled fast reactor (SFR) plant can occur due to a pipe leak or break. Accumulation of the sodium in a pool would allow the sodium to react with the atmosphere of the containment, such as oxygen, to cause a fire. Sodium fire is important to model because the heat addition and aerosol generation that occur. Any fission products trapped in the leaked sodium coolant may also be released into the containment, which can affect workers and the public if the containment is breached. This paper describes progress of an international collaborative research in SFR sodium fire modeling between the United States and Japan under the framework of the Civil Nuclear Energy Research and Development Working Group (CNWG). In this collaboration between Sandia National Laboratories (SNL) and Japan Atomic Energy Agency (JAEA), the validation basis for and modeling capabilities of sodium pool fires in MELCOR of SNL and SPHINCS of JAEA are being assessed. Additional model improvements for the sodium pool fire in MELCOR are discussed. The MELCOR results for the sodium pool fire model enhancement in MELCOR agreed well with the JAEA's F7 pool fire experiments and compared closely with SPHINCS.

KEYWORDS
Sodium pool fire, MELCOR, SPHINCS, Sodium-cooled fast reactor, Aerosol

1. INTRODUCTION

A sodium pool fire in the containment of a sodium-cooled fast reactor (SFR) plant can occur due to a pipe leak or break. This break may lead to the release of sodium spray droplets into the containment atmosphere where a sodium spray fire is possible. Further, any unreacted sodium droplets may fall onto the containment floor, possibly continuing as a sodium pool fire. An accumulation of the sodium in a pool can react with the oxygen in the containment atmosphere, causing a fire. Sodium fire is important to model because of the associated heat addition and aerosol generation . Any fission products trapped in the sodium released into the containment can affect workers and the public if the containment is breached.

The sodium fire phenomena have been captured in the nuclear reactor accident codes such as MELCOR and SPHINCS. MELCOR is a severe accident code developed by Sandia National Laboratories (SNL) for the U.S. Nuclear Regulatory Commission (NRC). SPHINCS is a sodium fire accident code developed by Japan Atomic Energy Agency (JAEA). Through the international collaborative research in the area of SFR sodium fire modeling between the United States and Japan, under the framework of the Civil Nuclear Energy Research and Development Working Group (CNWG), SNL and JAEA are working together to develop better modeling of sodium fire in their respected code development. This collaborative work, ongoing since 2016, which includes benchmark analyses of many sodium fires experiments that were done at SNL and JAEA.

This paper focuses the latest achievement in the enhancement on the sodium fire modeling in MELCOR for its validation using the JAEA's F7 series experiments for the sodium pool fire and including the code-to-code comparison to SPHINCS [1]. These enhancements were done in the MELCOR code input, rather than MELCOR software. MELCOR input allows a modeling capability via its powerful control function package [1]. The current sodium fire validation includes thermal-hydraulics and aerosol behaviors, which are greatly influenced by the conditions in the pool and its surroundings, especially including the substrate and atmosphere conditions. This paper describes the current state and enhancement of the sodium pool fire model in MELCOR and provides a brief description of the F7 experiments. In addition, this paper describes the validation study using MELCOR to simulate the F7 experiments including a discussion of the code-to-code comparison to SPHINCS.

2. SODIUM POOL FIRE MODEL

The initial sodium pool fire model in MELCOR has been adapted from CONTAIN-LMR, which was originally based on the SOFIRE II code [2]. The SOFIRE II model was developed from the results of legacy pool fire experiments. These tests concluded that the sodium burning rate was proportional to the oxygen concentration and was controlled by diffusion of oxygen to the pool surface through the convective boundary layer. This initial implementation of a MELCOR sodium pool fire model is parametric.

A mechanistic enhancement of the current model, to ensure broader applicability beyond the original testing basis of the parametric model, is an important motivation for this JAEA and SNL collaboration under the CNWG framework. As observed in the sodium pool fire experiments conducted at SNL [3], the progression of the sodium pool fire may depend on the oxide layers and other solidified materials at the pool surface. The inclusion of the rate-limiting oxide layer is a key model enhancement. In addition, the sodium pool fire experiments conducted at JAEA, such as the F-series tests, indicated that liquid sodium spreading impacts progression of sodium fires [4]. The F-series tests conducted at JAEA also measured suspended aerosol, which would be influenced by the amount of sodium by-products residing in the pool.

2.1. Current Model in MELCOR

The sodium pool fire model is described in greater detail, including model inputs, in the literature [4]. A summary of the model inputs for MELCOR is provided below.

To provide flexibility in the testing of uncertain inputs of the current pool fire model, many of the input parameters can be implemented as user-specified control functions. This greatly extends the flexibility of the model, enabling exploration of parametric uncertainties and alternate modeling approaches [5]. Sodium spreading on a surface can be explored within the framework of the control function infrastructure implemented to support the current pool fire model. The spreading of sodium will dynamically change the effective diameter of the pool on the spreading surface. Using control functions,

this record can be dynamically adjusted throughout the course of a simulation to represent the spreading of the sodium pool (i.e., the change in its diameter) in the integral MELCOR simulation. How the pool diameter changes can be represented by control function inputs defined as part of a MELCOR simulation input file, as discussed further in [4].

As shown in Table I for the current sodium pool fire model, there are several input parameters. Currently, these input parameters are entered as constants. A control function capability was added to each of these input parameters to easily permit the implementation of the model improvement. The improvement can be a correlation or equation. Implementation of an enhancement to the input parameter (DAB) for the oxygen diffusion coefficient model in the current work is investigated. The DAB parameter controls modeling of the oxygen diffusion to available sodium and thus enables a simulation to capture how reaction rates are altered due to the buildup of the oxide layers above the pool. This paper discusses the refinement of the oxygen diffusion correlation that can limit the rate of sodium consumption. In addition, the F7 experiments measured suspended aerosols. Aerosol formation and dynamics are influenced by many factors, including the amount of the sodium by-products rising from the pool fire. The updated input allows control functions to dynamically adjust the fractions of the sodium by-products such as Na_2O and Na_2O_2 as fNA$_2$O and fNa$_2$O$_2$, respectively in Table I.

Table I. Physics Input Parameters for the Current Sodium Pool Fire Model in MELCOR

Parameter	Description
FO2	Fraction of the oxygen consumed that reacts to form monoxide. The value 1.0-FO2 is the remaining oxygen fraction for the reaction to form peroxide.
FHEAT	Fraction of the sensible heat from the reactions to be added to the pool. The balance will go to the atmosphere.
FNA2O	Fraction of the Na_2O remaining in the pool. The balance will be applied to the atmosphere as aerosols.
FNA2O2	Fraction of the Na_2O_2 remaining in the pool. The balance will be applied to the atmosphere as aerosols.
TOFF	Model deactivation time. This is useful for modeling experiments.
DAB	Oxygen diffusion coefficient model switch. The default diffusion correlation will be used if a real value of greater than or equal to 0.0 is specified.

2.2. Model Improvement for MELCOR

This section describes the modeling improvement for the sodium pool fire in MELCOR. These improvements will be implemented as the series of control function inputs without modifying MELCOR. The reader should consult [1] for the translation of the model improvement from equations to control functions. See Table I for the input parameters to be modified as a control function variable so that the model enhancement can be implemented as inputs for MELCOR.

2.2.1 Oxygen Diffusion

This section describes the improvement of the treatment of oxygen diffusion through oxide layers at low temperature (< 600 ºC) (see Equation 1).

$$D_{diff} = \frac{\left(\frac{Sh}{L}\right)\left(\frac{D}{1+\delta/\Delta_l}\right)}{0.14\left(g\, S_c \frac{\beta}{\nu^2}\, |T_{surf} - T_g|\right)^{\frac{1}{3}}}, \quad (1)$$

where Sh is the Sherwood number, L is the pool diameter, D is the gas diffusion coefficient, δ is the oxide layer thickness, which is normalized by the characteristic length scale (Δ_l), g is the acceleration due to gravity, Sc is the Schmidt number, β is the coefficient of gas expansion, ν is the kinematic viscosity, T_{surf} is the sodium pool surface temperature, and T_g is the gas temperature. The gas diffusion coefficient is given by

$$D = \frac{6.4312 \times 10^{-5}}{P_g}\left[\frac{(T_{surf} + T_g)}{2}\right]^{1.823} \quad (2)$$

where P_g is the gas pressure. The Schmidt number is:

$$S_c = \frac{\nu}{D} \quad (3)$$

The coefficient of gas expansion, which expresses reciprocal of temperature is,

$$\beta = \frac{1}{0.5 \cdot (T_{surf} + T_g)} \quad (4)$$

The oxide layer thickness δ is calculated by the mass of Na_2O and Na_2O_2 in the pool. The thickness is the summation of these two by-products in the pool. The characteristic length scale (Δ_l) is employed to normalize the thickness in Equation (1).

$$\Delta_l = \left(\frac{D_{eff}}{D}\right)\Big/\left(\frac{Sh}{L}\right) \quad (5)$$

The Sh is given for turbulent flow regime flow conditions in a circular pool:

$$Sh = 0.16(GrSc)^{1/3} \quad (6)$$

Where Gr is the Grashof number and is given as:

$$Gr = \left(\frac{T_{surf} - T_g}{T_g}\right)\left(\frac{g}{\nu^2}\right)L^3. \quad (7)$$

Note that the denominator in Equation (1) is very similar to Sh in Equation (6) because the Sh with the constant 0.14 is used in the equation of pool combustion from where Equation (1) is derived. In order to be similar form as in Equation (7), the denominator of Equation (1) needs to be multiplied by L/L Substituting Equation (7) into the denominator of Equation (1) and assuming β cancels out T_g in Gr and approximate constant is like that of Equation (1). Finally, the denominator becomes Sh/L which can be cancelled out the Sh/L term in the nominator in Equation (1). Then, Sh/L in the nominator of the righthand side of Equation (1) cancels can be dropped out, which leaves. Then Equation (1) becomes

$$D_{diff} = \frac{D}{1+\delta/\Delta_l} \quad (8)$$

Equation (8) will be used in the control function for the DAB parameter in Table I.

2.2.2. Liquid Sodium Spreading

The spreading of the liquid sodium is an important phenomenon impacting the sodium fire intensity. In the literature [4], we have described this model in detail. A 1-dimensional (1-D) radial spreading model (a pancake model) is used to describe the liquid sodium behavior as it falls downward onto the center of the pool; it then spreads outward. The pancake spreading is influenced by both viscous and gravitational forces. The final radial spreading distance as implemented is shown below

$$R(t+\Delta t) = \sqrt[8]{R(t)^8 + C_1 \cdot \frac{g}{\mu \pi^3 \rho^2} m^3 \Delta t} \tag{9}$$

where μ, ρ and C_1 are the sodium viscosity, density, and empirical constant, respectively. Including the effect of solids in the liquid sodium, the enhanced sodium viscosity μ is given as the function of the fraction of the sodium oxides (ε) by:

$$\mu = \mu_0 \cdot \exp\left(2.5\, C_2 \cdot \varepsilon\right) \tag{10}$$

C_2 in Equation (10) is an empirical constant. The Ramacciotti correlation has been used extensively for modeling corium experiments, which has allowed determination of an appropriate C_2. μ_0 is expressed as Pa-s by [4]:

$$\mu_0 = \frac{3.24 \times 10^{-3} e^{508/T}}{T^{0.4925}} \tag{11}$$

The drop height of the sodium flow onto the pool surface is assumed to be very small, so that no heat transfer or reaction occurs during the drop to the pool. However, depending on the mass flow rate of the liquid sodium into the pool, the spreading rate on the floor (or pan, in experiments) can vary. As a simplification, it is assumed that the sodium fire does not influence the viscosity of the liquid and solid mixture, which is very different from the corium flow where the corium is becoming more viscous due to heat loss to the surroundings. The solids are generated from the sodium fire where sodium oxide by-products are formed and started to accumulate in the pool. As the solid fraction of the pool increases due to the buildup of solid oxide by-products, the viscosity of the mixture increases substantially. This viscosity and viscosity multiplier model are well described in the literature will eventually be incorporated [4].

Using the amount of sodium oxides in the pool, the volume solid fraction, ε is given by:

$$\varepsilon = \frac{\sum \frac{m_j}{\rho_j}}{\sum \frac{m_i}{\rho_i}} \tag{12}$$

Where both m and ρ are the mass and density of oxide material j, and sodium compound material, i in the pool. i also includes sodium liquid.

Because the spreading model presented here was adapted from MELCOR for the corium spreading, new empirical constants for Equations (9) and (10) must be determined to model the spreading of the liquid sodium with oxide solids. In addition, when the spreading front has sufficient solid buildup, the spreading is stopped. These equations for the sodium spreading will be implemented in the control function as MELCOR input.

2.2.3. Pool-to-Pan Heat Transfer

In the literature [4], we have identified a need for a quasi-two-dimensional (2-D) heat transfer model for a 1-D heat structure model in MELCOR to better characterize the heat transfer between the sodium pool and substrate or catch pan. The current 1-D heat structure model for the catch pan has just a single radial temperature node. This 1-D model assumes an infinite thermal conductivity radially. As a result, the heat loss from the pool to the catch pan is excessive until the pool reaches the edge of the catch pan.

The catch pan is physically heated to high temperature under the pool and remains at low temperature where there is no pool. Once the catch pan temperature under the pool becomes almost equal to the pool temperature, the heat transfer at this portion of the pan is suppressed. Consequently, the phenomenon requires a 2-D heat structure model of the catch pan. A 2-D heat structure model is being implemented into MELCOR for both cartesian and cylindrical heat structures. However, the cylindrical model is not yet completed. Consequently, a quasi-2-D model was developed using the 1-D heat structure model.

In the quasi-2-D model shown in Fig. 1, the catch pan is modeled using two temperature regions, under the pool ($T_{pan\text{-}1}$) and its outside ($T_{pan\text{-}2}$). Heat transfer between the pool and the catch pan ($q_{pool\text{->}pan}$) is calculated using $T_{pan\text{-}1}$.

$$q_{pool-pan} = (HTC)_{pool-pan} * (T_{pool} - T_{pan-1}) \quad (13)$$

where $(HTC)_{pool\text{-}pan}$ is the heat transfer coefficient between the pool and the catch pan. Then $T_{pan\text{-}1}$ can be defined.

$$T_{pan-1} = \frac{A_{pan}}{A_{pool}} T_{pan} + (1 - \frac{A_{pan}}{A_{pool}}) T_{initial} \quad (14)$$

These equations will be programmed as control function statements for heat exchange between the pool and the pan (see details in [4]).

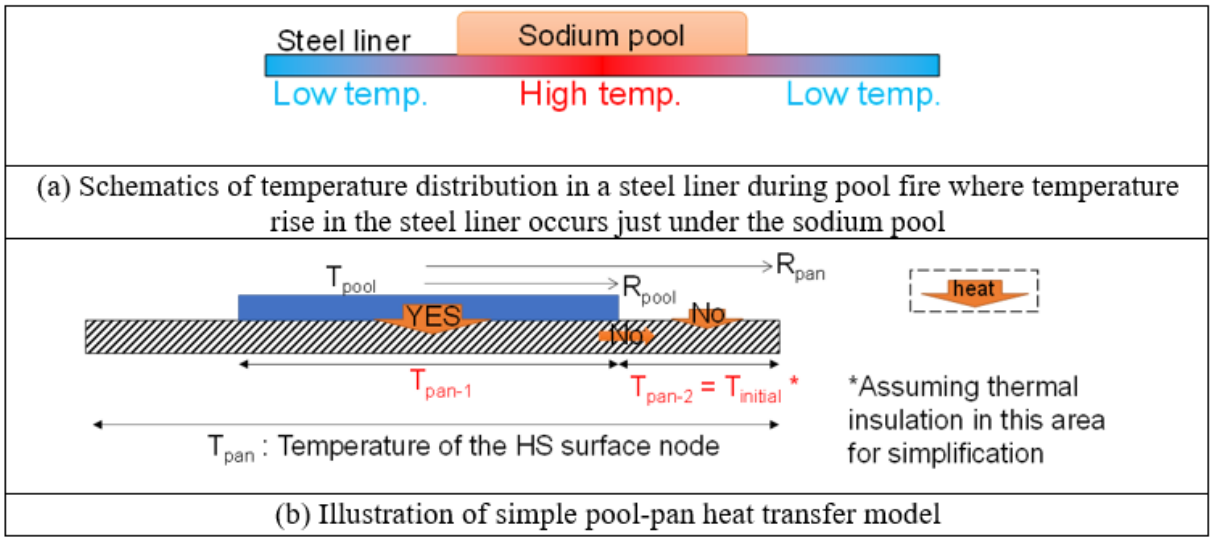

Figure 1. Temperature region in the pool-pan heat transfer model for 1-D heat structure

2.2.4. Pool Oxide Fractions

There are two pool oxide fractions in the current pool fire model: FNA2O and FNA2O2 for the fraction of sodium monoxide and sodium peroxide in the pool, respectively. As mentioned before, the release of the oxide from the pool corresponds to the amount of the oxide that has been cumulated in the pool. At the beginning of the pool fire, there are no oxides in the pool. It is expected that most of the newly formed oxides would be released in the atmosphere because there is no oxide crust to block or minimize their release. These phenomena may require a dynamic specification of FNA2O and FNA2O2 in the model rather than a constant value for the entire fire scenario.

To analyze the effect of the sensitivity of FNA2O and FNA2O2 values on the suspended aerosol, various constant values of FNA2OX for FNA2O and FNA2O2 were input to the MELCOR pool fire model. This sensitivity study assumes that the aerosol released from the pool is a strong function of the amount of oxides in the pool as postulated above. So, a range from 0.1 to 0.9 of FNA2OX constant values were input to the MELCOR to observe the amount of suspended aerosol in the problem. The sensitivity study showed that small a constant value of FNA2OX would yield large, suspended aerosol concentration results, while large FNA2OX constant value would yield small, suspended aerosol concentration results. Consequently, the amount of FNA2OX impacts the rate of aerosol release versus retention in the pool. It is assumed that FNA2OX has the following form:

$$\mathrm{FNA2OX} = a_1 \cdot \varepsilon^{a_2} + a_3 \cdot \varepsilon + a_4 \qquad (15)$$

where a_1 to a_4 are the coefficients. Equation (15) will be implemented into a series of control functions for the FNA2O and FNA2O2 parameters as shown in Table I.

2.3. Sodium Pool Fire Model in SPHINCS

SPHINCS is developed by JAEA as a sodium fire analysis code with a lumped mass model for control volumes and a 1-D flow network model that is like MELCOR [6]. The flame sheet model is used for the pool combustion. This model employs four conservation equations in terms of mass and energy transfer on the flame sheet layer with zero thickness: molar flux of sodium vapor and oxygen (or water vapor),

heat transfer between the pool and the flame sheet, and heat transfer between the atmosphere and the flame sheet. By solving these equations, source terms of mass and energy transportation due to pool fire are obtained.

SPHINCS also has a model for the effect of the oxide layer on the pool combustion considering the mass fraction of the oxide in the sodium pool. The pool combustion rate is multiplied by the liquid sodium fraction over the total pool mass that includes the mass of the oxide. The multiplier is 1.0 when there is no oxide as well as MELCOR's model described in Equation (8). The sodium pool spreading in SPHINCS is modeled to be influenced by the surface tension and the gravitational force. Its spreading is almost constant except for the change in the sodium physical properties, which depend on temperature. In order to restrict the pool spreading, the maximum pool area can be specified in the input deck. Once the pool area reaches the maximum value, the expansion of the pool stops and the pool height starts increasing. Heat transfer between the pool and the floor is calculated in the 2-D system. Since the computational mesh is divided into ring-shaped coordinate system, SPHICNS can accurately simulate the temperature distribution in Fig. 1(a).

3. MELCOR VALIDATION STUDY

The MELCOR validation study consists of benchmarking the sodium pool fire model enhancements against JAEA's F7-1 and F7-2 tests [7], including the code-to-code comparison to JAEA's SPHINCS code. This section presents a brief description of the F7 test experiments of F7-1 and F7-2, followed by the calculation results of MELCOR and SPHINCS, and a discussion of the results.

3.1. F7 Test Description

The test apparatus, shown in Fig. 2, consists of the stainless-steel vessel, the liquid sodium discharging system, the stainless-steel catch pan, the thermal insulator, the air ventilation (purge) line, and the measurement system. The test vessel is about 2.2 m in height and 1.3 m in diameter. The key difference between the F7-1 and F7-2 tests is the height of the nozzle exits, which are located at 0.1 m and 1.5 m from the catch pan, respectively. The thickness and area of the catch pans are 6 mm and 1 m^2, respectively. The catch pan is attached to two 50 mm layers of thermal insulation. The liquid sodium is discharged with the average leak rate of 3.3 g/s for 1,500 seconds. The liquid sodium falls with a column shape and forms a pool on the catch pan. The final areas of the sodium pool are 0.28 m^2 for F7-1 and 0.30 m^2 for F7-2, respectively. The air in the vessel is ventilated with a steady flow of approximately 3.0 m^3/min. The test conditions are summarized in Table II.

The experimental temperature measurements of the vessel surface, the atmosphere, the pool, the bottom surface of the catch pan, and the surface between the two-thermal insulation layers were monitored with multiple thermocouples. The concentrations of oxygen, hydrogen, and aerosolized material were also measured in this test. The measured values used for comparison with the computational results were obtained from the experiment test report [7].

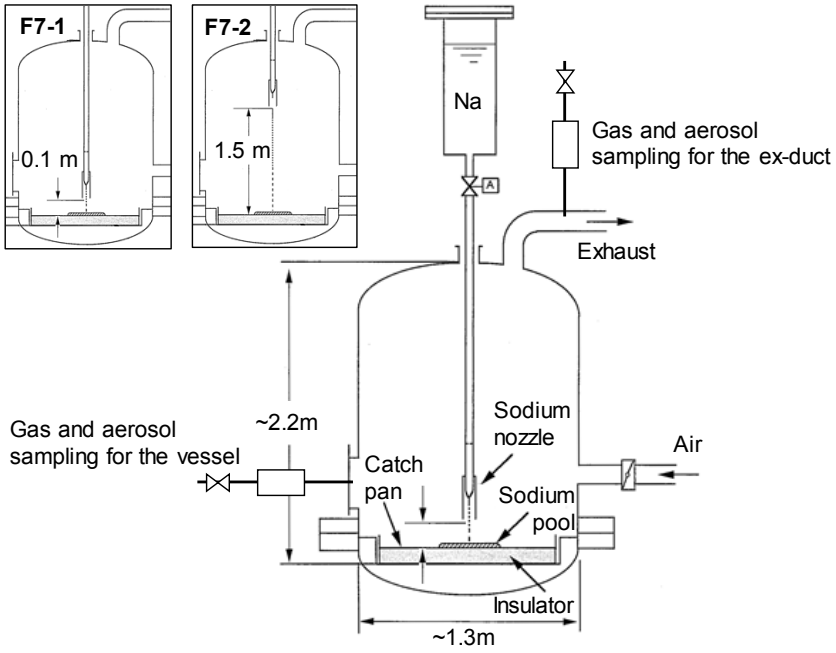

Figure 2. Test apparatus for F7-1 and F7-2 tests [1]

Table II. Test conditions of F7-1 and F7-2 tests [1]

Parameter	F7-1	F7-2
Sodium temperature	505°C	
Sodium leak form	Column	
Sodium leak height from catch pan	0.1 m	1.5 m
Sodium leak duration	Approximately 1,500 s	
Average sodium leak rate	3.3 g/s	
Total leak quantity of sodium	4.94 kg	
Oxygen concentration (initial)	20.8%	20.7%
Atmosphere temperature (initial)	12.7°C	19.6°C
Atmosphere relative humidity	49.2%	71.5%
Ventilation flow rate	Approximately 3.0 m^3/min	

3.2. MELCOR Model

Like the previously developed MELCOR model [4], the MELCOR model for simulating the F7 test used three control volumes and the two flow paths, as shown in Fig. 3. A similar set up was used for SPHINCS. The spray and pool fire occur in the control volume "FRAT," which corresponds to the vessel of the F7 tests. The "PREENV" and "ENV" correspond to the environment as shown in Fig.3. The velocity at the exit flow path to "ENV" was set to 5.74 m/s throughout the computation, which corresponded to 3.0 m^3/min in the exit pipe with a cross-sectional area of 8.71×10^{-3} m^2. The inlet flow condition from "PREENV" was specified as a pressure boundary condition with free flow in accordance with the test condition. There are three heat structures: the rectangular "top head," the cylindrical "wall," and the rectangular "bot head." The "top head" and "side wall" heat structures are stainless steel. The "bot head" heat structure is divided into the carbon steel pan and the outer thermal insulation layer. The

surface area of the "bot head" is 1.0 m^2. Each heat structure is divided into several conduction mesh nodes in the thickness direction. There is natural convection and radiation heat transfer between the surface of each heat structure to the pool and the atmosphere. The input parameters for heat transfer and sodium fire computation are summarized in Table III and Table IV, respectively. The radiation view factors of the top head and wall are specified according to the ratio of the solid angle. The initial temperature of the atmosphere and all the heat structures were set to the same value. The spray height is the only difference in the MELCOR model between F7-1 and F7-2, where 0.1 m and 1.5 m are used, respectively. As shown in Table IV, a sodium spray fire model was activated for both tests, which may not reflect the column formation observed in the experiments. Since the spray model is based on a surface area of the droplet for the reaction, this may overpredict the amount the sodium reacted before falling onto the pool. Since the spray height is low, the contribution by the spray fire model may not be significant. The control functions for the enhancement described in Section 2.2 are not given in this paper. A description of the control functions for these enhancements are fully provided in Ref. [1].

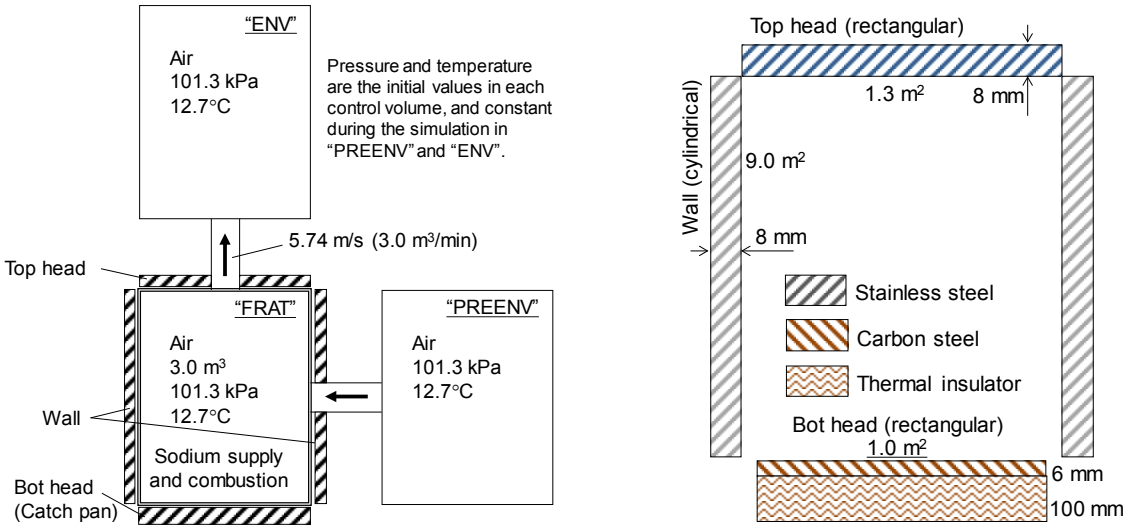

(a) Control volumes and flow paths (b) Heat structures

Figure 3. MELCOR and SPHINCS input model setup

Table III. Computational conditions of heat transfer for MELCOR

Natural convection heat transfer coefficient		6.08 W/(m^2-K)*
Radiation model		Gray gas model
Emissivity of heat structure surface		0.90
Emissivity of pool surface		0.98
View factor	Top head	0.04
	Wall	0.96
	Bot head	0.00

* HTC for the "bot head" HS was modified to be given by the MELCOR's internal convective heat transfer model using with the "CalcCoefHS" option.

Table IV. Computational specifications of sodium spray and pool fire for MELCOR

Spray fire	Height	0.1 m for F7-1, 1.5 m for F7-2
	Droplet diameter	0.0045 m
	FNA2O2	1.0
	Time step	Terminal velocity model
Pool fire	FO2	0.6
	FHEAT	0.6
	FNA2O	See Section 2.2.4, modeled as CF*
	FNA2O2	See Section 2.2.4, modeled as CF*
	TOFF	3600.0 s
	DAB	See Section 2.2.1, modeled as CF*

*CF as control function arguments, and as MELCOR inputs, see [1] for the control function arguments used.

3.3. Simulation Results and Discussions

The MELCOR result is compared with the result by JAEA's code SPHINCS. The comparison results of the two codes are shown in Fig. 4. As shown in Fig. 4 (b), the pool combustion rate shows a similar result until 600 s. After 600 s, the SPHINCS result starts to decrease because pool spreading stops, while the pool in the MELCOR simulation is predicted to continue spreading during sodium discharge. The difference in the catch pan temperature predicted by both codes also remains relatively large. The aerosol concentration also has a difference with SPHINCS when the oxide fraction to the pool is constant at 0.75.

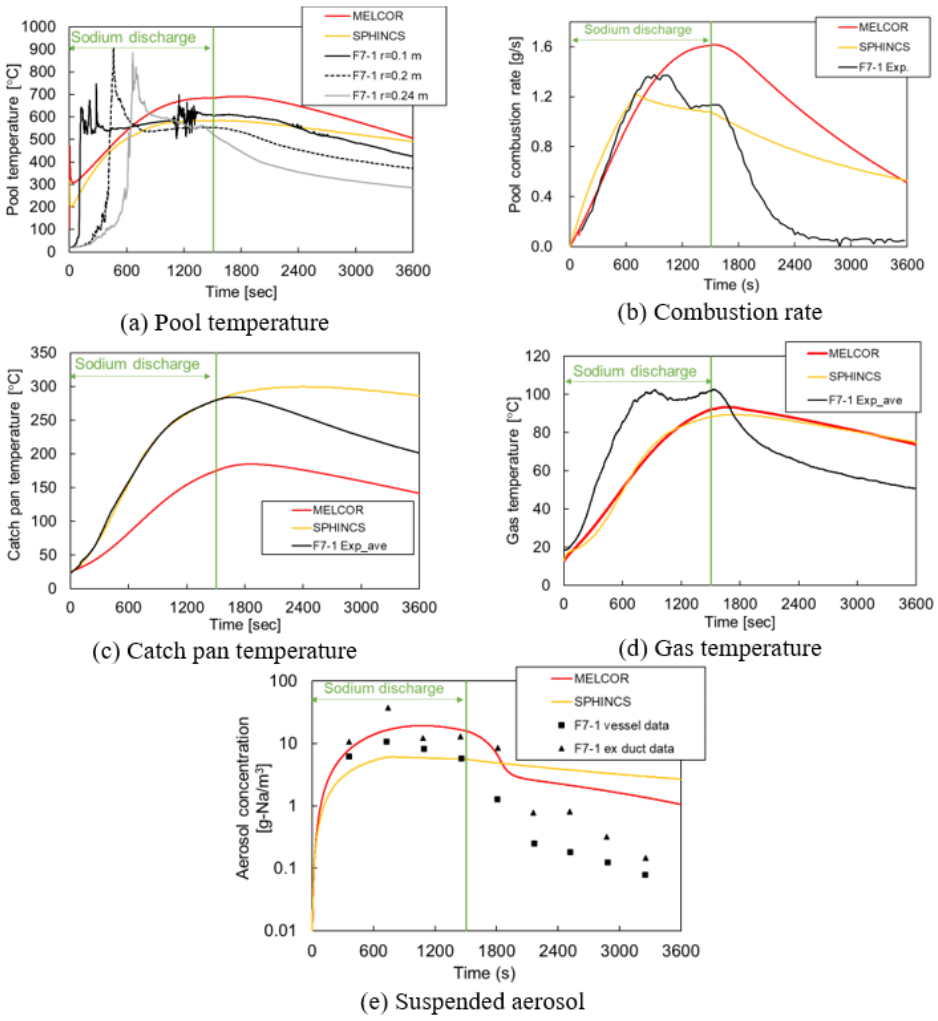

Figure 4. F7-1 Results and code-to-code comparison

Figure 5 shows the F7-2 result in the MELCOR model comparing with the SPHINCS result and t he F7-2 test data. The spray height is the key difference between F7-1 (0.1 m) and F7-2 (1.5 m). Spray combustion becomes more significant in F7-2 than F7-1. The rapid decrease in the gas tem perature at 1500 s shown in Fig. 5

Figure (d) is expected to be caused by termination of spray combustion. The comparison of the te mperature with SPHINCS and the F7-2 test has no noticeable difference from the F7-1 result. Fig ure 5(e) shows the F7-1 aerosol concentration results are similar to the F7-1 results.

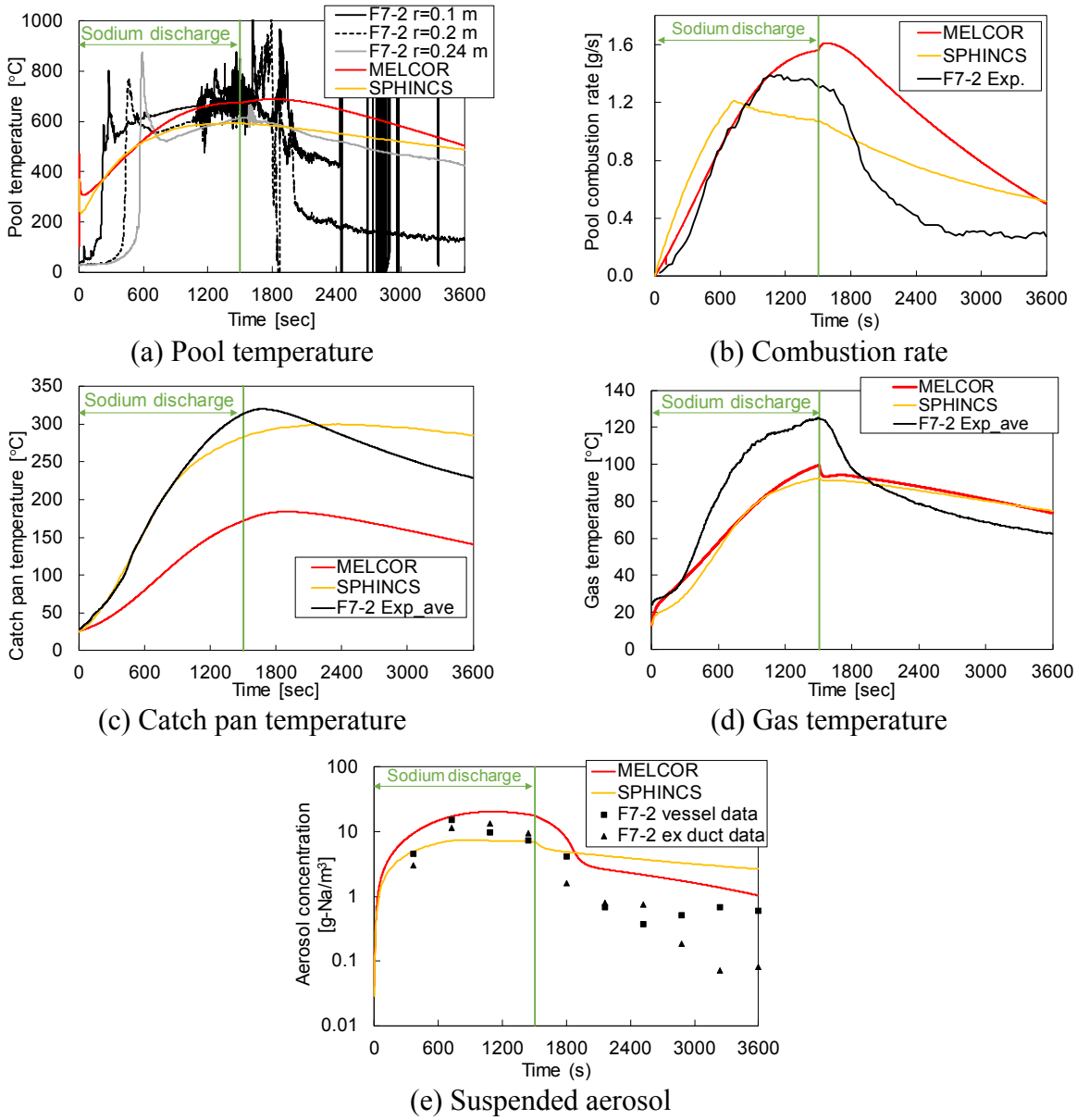

Figure 5. F7-2 Results and code-to-code comparison

4. CONCLUSIONS

This paper presents the progress of the sodium fire modeling collaborations between SNL and JAEA on validating MELCOR's sodium pool fire model enhancement. Both F7-1 and F7-2 pool fire experiments of JAEA were used for the validation, along with the code-to-code comparison with JAEA's SPHINCS code. The modeling improvement allows better matching with the experimental results by providing realistic models for input parameters for the MELCOR sodium pool fire model. Additionally, the code-to-code comparison between MELCOR and SPHINCS demonstrated significant improvement in there agreement on many key parameters.

In conclusion, the validation study on MELCOR's sodium pool fire model has progressed. Additional MELCOR input deck refinement is recommended to better capture the spatial effects observed in the post-examination of the samples in the F7-1 and F7-2 experiments.

ACKNOWLEDGMENTS

Sandia National Laboratories is managed and operated by National Technology and Engineering Solutions of Sandia, LLC under DOE NNSA contract DE-NA0003525. This work is supported by DOE Work Package: RD-21SN040307. The authors also would like to extend thanks to David Luxat of SNL and Akihiro Uchibori of JAEA for providing suggestions and improvements for this research. Finally, the authors appreciate the K.C. Wagner of SNL for peer reviewing this paper.

REFERENCES

1. D.L.Y. Louie and M. Aoyagi, "Sodium Fire Collaborative Study Progress -CNWG Fiscal Year 2021," SAND2021-15469, Sandia National Laboratories, Albuquerque, NM, USA (2021)
2. P. Beiriger, J, Hopenfeld, M. Silberberg, R.P. Johnson, L. Baurmash, R.L. Koontz, "SOFIRE II User Report," AI-AEC-13055, Atomics International, Canoga Park, CA (1973).
3. T.J. Olivier, T.K. Blanchat, V.G. Figueroa, J.C. Hewson and S.P. Nowlen, "Metal Fires and Their Implications for Advanced Reactors Part 3: Experimental and Modeling Results," SAND2010-7113, Sandia National Laboratories, Albuquerque, NM, USA (2010).
4. D.L.Y. Louie and M. Aoyagi, "Sodium Fire Collaborative Study Progress–CNWG Fiscal Year 2020, SAND2021-0136," Sandia National Laboratories, Albuquerque, NM, January 2021.
5. L.L. Humphries, B.A. Beeny, F. Gelbard, D.L. Louie and J. Phillips, "NAC Package Reference Manual" in MELCOR Computer Code Manuals, Vol. 1: Users Guide Version 2.2.11932, SAND2018-13559O, Sandia National Laboratories, Albuquerque, NM, USA (2018).
6. A. Yamaguchi, T. TAkata, Y. Okano, Numerical Methodology to Evaluate Fast Reactor Sodium Combustion, *Nuclear Technology*, **136**, pp.315-330 (2001).
7. S. Futagami, M. Nishimura, K. Kawata, H. Ishikawa, S. Miyahara, Sodium Pool Combustion Test Run-F7 (Interim Report), PNC TN9410 98-074, Power Reactor and Nuclear Fuel Development Corporation, Oarai, Japan (1998).